Article

Functional Connectivity of Paired Default Mode Network Subregions in Retinal Detachment

Ting Su[1,2,*], Yong-Qiang Shu[3,*], Kang-Cheng Liu[1], Lei Ye[1], Ling-Long Chen[3], Wen-Qing Shi[1], You-Lan Min[1], Xiao-Wei Xu[1], Qing Yuan[1], Pei-Wen Zhu[1], and Yi Shao[1]

[1] Department of Ophthalmology, The First Affiliated Hospital of Nanchang University, Jiangxi Province Clinical Ophthalmology Institute, Nanchang, Jiangxi, China
[2] Eye Institute of Xiamen University, Fujian Provincial Key Laboratory of Ophthalmology and Visual Science, Xiamen, Fujian Province, China
[3] Department of Radiology, The First Affiliated Hospital of Nanchang University, Nanchang, Jiangxi, China

Purpose: To explore the difference of the default mode network (DMN) in patients with retinal detachment (RD) by the study of the resting state functional connectivity (rs-FC).

Methods: A total of 30 patients with RD (16 men, 14 women) and 30 similarly matched normal controls (NCs) were examined and recorded with rs-fMRI. The DMN was divided into eight core regions, and each rs-FC map of each subregion was obtained. The receiver operating characteristic (ROC) curve was performed to classify the mean FC values of RD patients from NCs, and the interrelationships between the FC and each region were evaluated with Pearson's correlation analysis.

Results: Compared with NCs, there were significantly increased FC in the left medial temporal lobe (MTL.L) and posterior cingulate cortex (PCC), MTL.L and left hippocampus formation (HF.L), MTL.L and HF.R, MTL.L and left inferior parietal cortices (IPC.L), MTL.L and IPC.R in the RD group ($P < 0.05$). Nevertheless, no correlation between the FC values of each paired region and the manifestations was found in the RD group. ROC curve analysis showed that the accuracy of the area under the curve was excellent in MTL.L-HF.R and MTL.L-IPC.R and less reliable in MTL.L-PCC, MTL.L-HF.L, and MTL.L-IPC.L.

Conclusions: The visual function impairments of RD patients were closely related to the DMN functional connections, which provided insight into the neural variation in RD patients and assisted in revealing the potential mechanisms of RD.

Translational Relevance: This study provided insight into the neural variation in RD patients and assisted in revealing the potential mechanisms of RD.

Introduction

Retinal detachment (RD) is a common acute blindness eye disease and refers to the separation of retinal nerve epithelium from pigment epithelium; late stage RD can cause cataract, atrophy of eyeball, chronic uveitis, posterior synechia of the iris, and even blindness.[1] The most common form of RD is perforated RD.[2] It is reported that rhegmatogenous RD can occur at all ages, and even earlier in high myopia or other susceptible populations (such as trauma and vitreous detachment).[3] The most com-

mon patients are approximately 55 to 59 years old, with an incidence of about 5.25/10,000.[4]

Ultrasonography is effective in diagnosing RD, but it is relatively rough. It is difficult to make a good judgment of the extent and severity of RD.[5] Optical coherence tomography has been widely used in ophthalmology because of its noninvasiveness and high resolution. By providing cross-sectional images of the retina, we can quantitatively and qualitatively analyze the condition of RD to a certain extent, so as to make an effective diagnosis.[6] However, currently, more attention is paid to the related changes in the

eyes of RD patients, and the irreversible changes in the visual center of the visual disorders in patients with RD have not been systematically studied. The related neural mechanism is not very clear, and it is difficult to make a more accurate judgment. Therefore, the relevant research has become a hot topic in the field of neuroscience. It is related to the choice of RD diagnosis and treatment and even plays a guiding role in prognosis.[7]

Although there are some studies on visual cortex changes, they mainly focused on methods based on the visual evoked potential (VEP), horseradish peroxidase, immunofluorescence contrast agent, and magnetic resonance spectroscopy (MRS).[4] With the development of neural imaging technology related to structure and function, visual-related examination is no longer limited to VEP, MRS.[5] More and more techniques have been applied to the research of neural function and brain structure. Functional magnetic resonance imaging (fMRI) is a commonly used brain function detection technology in the field of brain imaging. Resting state functional magnetic resonance imaging (rs-fMRI) can assess brain activity changes. It can be used to judge brain activity and tissue patterns in the nontask state by resting state signals and functional responses, so as to examine the changes in the brain's functional tissues to better understand the mechanism of disease in brain tissue.[6,7] At the same time, by analyzing the functional connectivity of brain in both people with normal eyes and patients, we can reveal the abnormal brain function caused by the disease to some extent.

The default mode network (DMN) studied in this paper was first analyzed by Grecius and others[1] through functional connection. The main nodes included the bilateral parietal cortex, the posterior cingulate cortex (PCC), the prefrontal lobe, and the medial prefrontal lobe (medial prefrontal cortex, MPFC). This method mainly investigated the degree of synchronous activity of low-frequency blood oxygen signals in different regions of the brain in the quiet state. The synchronism of neural activity was conjectured by the synchronous activity of blood oxygen signal. The main index was the number of phase relations on the time sequence (time series) signal between the brain regions. This method could be used to study the functional integration between the brain regions.[2] The usual way was to set a seed point (seed), then calculate the functional connectivity strength in the brain regions.[3] In contrast to the research on the maintenance and execution functions of other networks, more and more studies of various

diseases have begun to explore the DMN changes. Some studies have found that DMN may be related to mental activities such as self-awareness, situational memory, planning, and imagination. Through the study of DMN, the production and development of related diseases can be investigated from multiple perspectives and may be helpful in assessing the curative effect and prognosis of disease treatment. The brain needs multiple brain regions to participate in the process of information processing, and functional connectivity is an effective way to study collaborative work between different brain regions. Therefore, we hope to explore the neural activity and neural mechanism of RD patients through the study of DMN functional connectivity of RD patients with fMRI.

Materials and Methods

Experimental Subjects

The patients from the ophthalmology department of the First Affiliated Hospital of Nanchang University were recruited in the study. Thirty patients with RD were treated as the RD group and 30 were in the control group. The visual acuity, intraocular pressure, slit lamp anterior segment, and fundus examinations were carried out. Inclusion criteria of RD group were as follows: (1) age 20 to 70; (2) timely follow-up; (3) unilateral idiopathic RD patients with one or two retinal tears according to ocular ultrasound; (4) no other eye diseases (cataract, glaucoma, optic neuritis, macular disease, etc.); (5) range of RD no more than two quadrants. Exclusion criteria of RD group were as follows: (1) serious complications such as vitreous blood and retinal macular degeneration; (2) history of ocular trauma; (3) patients with previous history of eye surgery or RD patients who had received laser treatment; (4) mental illness (such as depression, etc.) or nonmatched recipients; (5) amblyopia. All normal controls (NCs) met the following criteria: (1) with best-corrected visual acuity (VA) ≤ 0 LogMAR; (2) no deformities in the brain parenchyma on MRI; (3) no psychiatric disease; (4) capable of MRI examination (no cardiac pacemaker or implanted metal devices, etc.).

The study was approved by the medical ethics committee, First Affiliated Hospital of Nanchang University, and followed the Helsinki declaration. Consent was obtained from all subjects and written informed consent was signed.

Table 1. Information About MRI Parameters

Data Acquisition	Echo Planar Imaging Sequence	Brain Volume Sequence
Patient		
Sex		
Male	16	16
Female	14	14
Age, average range	51.40 ± 7.72	51.40 ± 7.72
Scan parameters		
Repetition time/echo time	2000/30 ms	1900/2.26 ms
Thickness/gap	4/1.2 mm	1/0.5 mm
Matrix	64 × 64	256 × 256
Field of view	230 × 230 mm	250 × 250 mm
Flip angle	90°	90°

MRI Data Acquisition

The data were collected with the 3.0T MRI system (Siemens, Munich, Germany) from the First Affiliated Hospital of Nanchang University. During the operation, the patient was instructed to close the eyes and keep awake, and the patient was tested after the head was fixed. The information and parameters are shown in Table 1.

The Preprocessing of fMRI Data

Data were preprocessed using Mathworks software (MATLAB2010a; Mathworks, Natick, MA) and MRIcro software (available free of charge from the University of South Carolina, CRNL, www.MRIcro.com). To obtain the image at a stable system, the first 10 time-point images were removed. The MATLAB2010a (Mathworks) advanced version of the rs-fMRI data-processing assistant (DPARSFA; available free of charge from the R-fMRI Network, http://rfmri.org/DPARSFA) was used to analyze the rs-fMRI data. Time correction and head motion correction of slice collection was completed using Friston six-head motion parameters, including the translation of each direction and the rotation angle of each axis. The artifact light source (multiple linear regression method) was removed, including head moving signal, cerebrospinal signal, whole brain signal, white matter signal.[4,5] The image was standardized using Montreal neurology Institute (MNI) EPI Template.[6] Resampling, using $3 \times 3 \times 3$ mm^3 voxel, and spatial smoothing was done, with half width of 6 mm. Bandpass filtering was 0.01 to 0.08 Hz.

DMN Subregions and Resting State Functional Connectivity (rs-FC) Analysis

According to previous studies, DMN was divided into eight core regions. The average time series of these eight regions were defined by placing spherical seeds (6-mm radius) and then extracted from each subject. In

Table 2. Demographics and Clinical Measures by Group

Data Acquisition	RD	NC	t	P
Sex			N/A	>0.99
Male	16	16		
Female	14	14		
Weight, kg	67.17 ± 3.21	66.93 ± 4.42	0.23	0.82
Age, y	51.40 ± 7.72	51.17 ± 6.95	0.12	0.90
Handedness	30 R	30 R	N/A	>0.99
Duration, d	24.05 ± 19.61	N/A	N/A	N/A
Best-corrected VA-RD eye, logMAR	1.50 ± 0.54	N/A	N/A	N/A
Best-corrected VA-contralateral eye, logMAR	0.49 ± 0.57	N/A	N/A	N/A

There were significant differences found in gender, weight, age, and handedness ($P > 0.05$). N/A, not applicable; R, right.
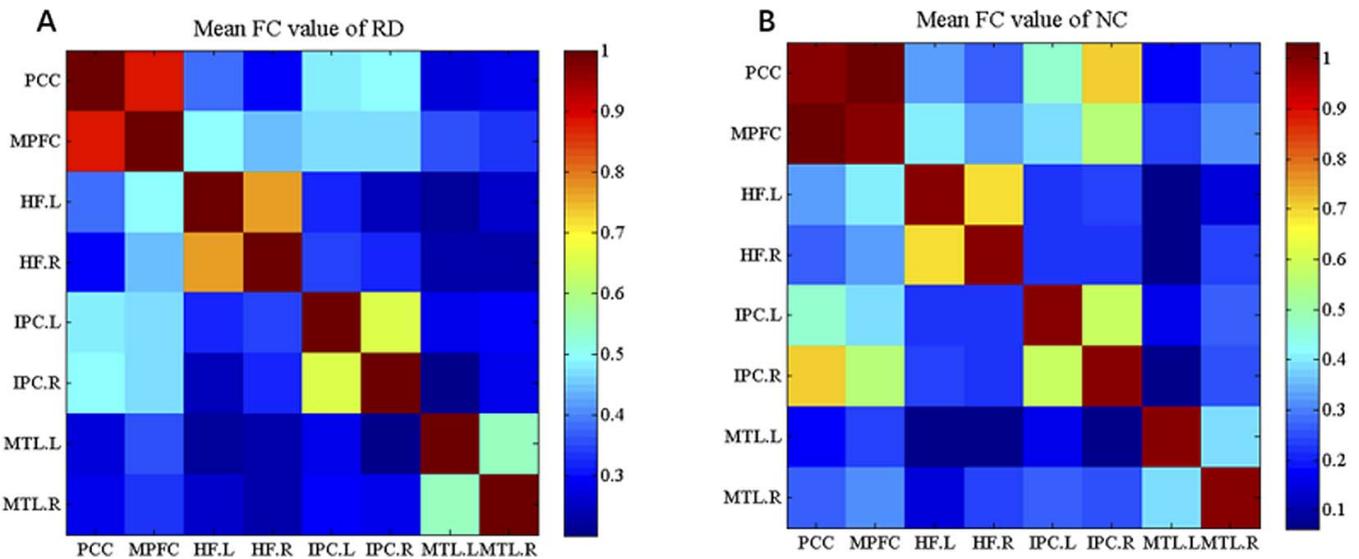
Figure 1. The correlation matrix of subregions of the mean time series of DMN. (A) The correlation matrix of the subregions in the mean time series of the RD group; (B) the correlation matrix of the subregions in the mean time series of the control group. Note: The photo represents DMN as the result of the subregions' FC. Different colors represent different connection coefficients. L, left; R, right.

order to study the relationship between FC and its strength, Pearson correlation coefficients were calculated and analyzed by Fisher's r-to-z transformation.

Statistical Analysis

Statistical software (SPSS16.0; SPSS, Chicago, IL) was used to analyze the data, and the independent sample t test was used to compare the demographic and clinical data between the two groups. The difference was statistically significant when $P < 0.05$. To classify the FC values in distinct paired cerebrum regions of the RD subjects separate from NCs, the receiver operating characteristic (ROC) curve method was performed.

Results

Demographics and Visual Measurements

There was no significant difference between the age ($P = 0.903$) and weight ($P = 0.816$). The best-corrected VA of the RD eye was 1.50 ± 0.54 logMAR, the best-corrected VA of contralateral eye was 0.49 ± 0.57 logMAR, and the average duration of RD was 24.05 ± 19.61 days. Details are presented in Table 2.

FC Value Differences Between NC and RD

The correlation coefficient was measured for each pairwise region. As shown in Figure 1, the FC

results of DMN were presented as correlation matrices and interrelated graphs for visualization in the RD and control group. The regions of DMN were closely related, and there was significantly increased FC in some paired regions in RD group when compared with NCs, including the left medial temporal lobe (MTL.L) and PCC ($t = 2.502$, $P = 0.017$), MTL.L and left hippocampus formation (HF.L) ($t = 2.147$, $P = 0.038$), MTL.L and HF.R ($t = 2.708$, $P = 0.010$), MTL.L and left inferior parietal cortices (IPC.L) ($t = 2.061$, $P = 0.046$), MTL.L and IPC.R ($t = 2.586$, $P = 0.014$) (Fig. 2). However, no correlation between the FC values of each paired region and the manifestations was found in the RD group ($P > 0.05$).

ROC Curve

We speculated that the differences of FC values could be potentially useful diagnostic markers to distinguish the RD group from the NCs. The ROC curve method was performed to verify this assumption, and the mean FC values of the distinct paired cerebrum areas were collected and analyzed. The individual areas under the curve (AUCs) of FC values in different paired regions were as follows: MTL.L-PCC (0.642, $P = 0.123$), MTL.L-HF.L (0.665, $P = 0.074$), MTL.L-HF.R (0.730, $P = 0.013$), MTL.L-IPC.L (0.628 $P = 0.168$), MTL.L-IPC.R (0.763, $P = 0.005$) (Fig. 3)
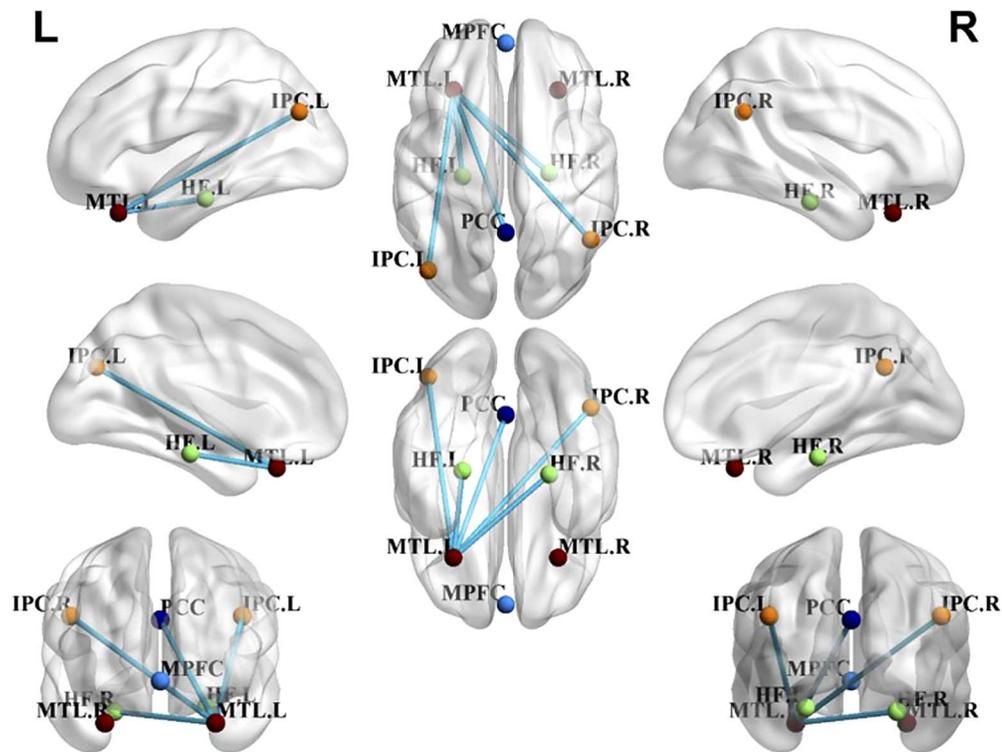
Figure 2. The different FC of the DMN between the RD and NC group. There were significant differences between RD and NC subjects. The different colored *dots* represent different nodes; the *blue lines* denote stronger correlations in RD group at the threshold. *P* < 0.05.

Discussion

As the most complex human network architecture, the brain is an important research subject in cognitive science, and it can be studied by analyzing its function and structure through brain-imaging technology. The technology for rs-fMRI is blood oxygen level–dependent, which is noninvasive, accurate, and direct. It is used to reflect the activation of the brain when stimulated or an action executed and demonstrates the stimulated area and the intensity and duration of the mental activity produced in the cerebral cortex. The functional advantages of each brain region can also be identified, and these studies are also more in-depth.[7] A large number of studies have shown that low-frequency oscillations occur in the resting state of human brain, which may be related to the occurrence and development of certain diseases.

For many years, many studies on the neurologic mechanisms of ophthalmologic diseases have adopted psychophysical methods to understand the mechanism of information sampling and coding in visual cortex neurons.[8–10] With the progress of technology, the neural mechanism of visual impairment of ophthalmologic diseases was found to be closely related to the spatial characteristics of neurons in the V1 area of the visual cortex, or even many regions of the visual cortex, and was related to the dysfunction of the functional connection between neurons.[11–13] RD patients have various visual defects, and the abnormal number of neurons in the visual cortex and the spatial characteristics cannot explain the results of physical testing. Because of the complex structural and functional connections between different brain regions, DMN can also get information from the external environment.[14,15] By detecting the FC of DMN, we found that the FC of MTL.L-PCC, MTL.L-HF.L, MTL.L-HF.R, MTL.L-IPC.L, and MTL.L-IPC.R in RD patients increased significantly with impaired visual function (Fig. 4). Studies have pointed out that diseases can cause changes in certain connections in the brain region.[16] The results of our study showed that when RD occurred, the synchronous dysfunction of brain activity in the brain hindered the information connection of the brain regions to a large extent. At the same time, our findings were consistent with earlier conjectures proposed by electrophysiologic research.

In our study, the FC of the MTL.L-PCC, MTL.L-HF.L, MTL.L-HF.R, MTL.L-
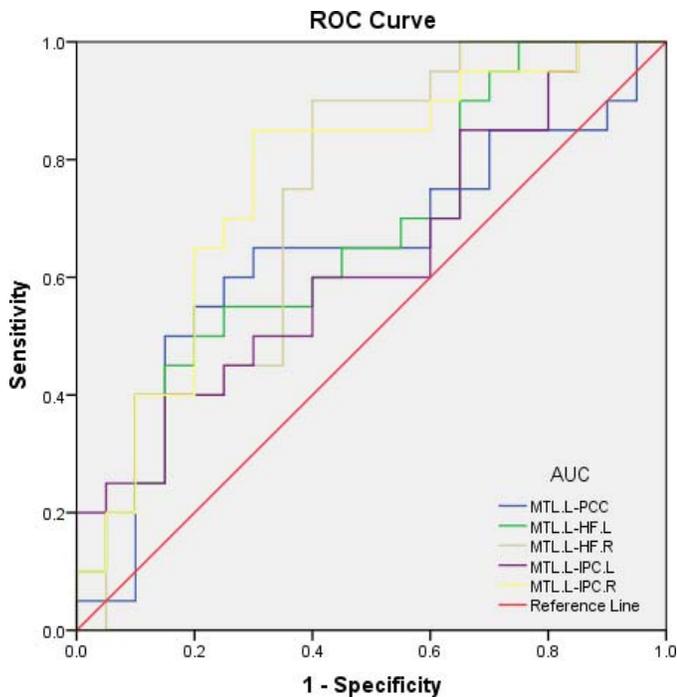
Figure 3. ROC curve analysis of the FC values in each paired subregion. The area under the ROC curve for MTL.L-PCC was 0.642 ($P = 0.123$; 95% CI: 0.464–0.821); MTL.L-HF.L, 0.665 ($P = 0.074$; 95% CI: 0.496–0.834); MTL.L-HF.R, 0.730 ($P = 0.013$; 95% CI: 0.569–0.891); MTL.L-IPC.L, 0.628 ($P = 0.168$; 95% CI: 0.454–0.801); MTL.L-IPC.R, 0.763 ($P = 0.005$; 95% CI: 0.610–0.915). CI, confidence interval.

IPC.R increased significantly. Therefore, we speculated that RD not only affected the visual field of the retina, but also altered its function in the visual system in various degrees. Previous research has demonstrated that the anterior and lower lobules of the wedge and the visual space are related to perceptual processing, extraction of situational memory, and self-consciousness.[17] The metabolism is very active in the resting state and is considered to be involved in the composition of DMN. FC measures the temporal correlation of DMN, while the low-frequency oscillation of brain neurons has time consistency in FC. DMN is mainly divided into four parts,[18] including the posterior cortex, the posterior cerebral cortex, the ventromedial cortex of the prefrontal cortex, and the dorsal cortex of the prefrontal cortex. The middle and posterior cortex areas mainly include cingulate gyrus, the precuneus, and the corporis callosi splenium. This area is one of the most important regions of the human brain energy metabolism, which is mainly related to the information processing of visual space. Studies have shown that the human visual system uses the striate cortex as the initial input and divides the ventral and dorsal bundles. The neurons in the ventral pathway respond to the characteristics of color and shape and deal with the information of object recognition. The neurons in the dorsal pathway react to the characteristics of the velocity and direction of the stimulus and deal with
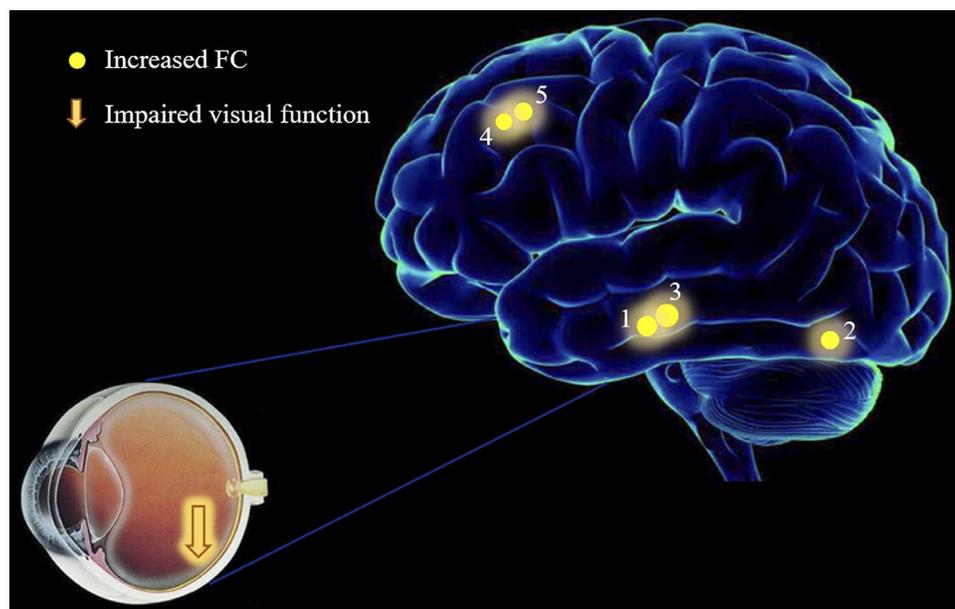

Figure 4. The rs-FC results of DMN in the RD group. Compared with the control group, the rs-FC of PCC was increased to various extents: 1-HF (L) ($t = 2.502$, $P = 0.017$); 2-MTL (L) ($t = 2.147$, $P = 0.038$); 3-HF (R) ($t = 2.708$, $P = 0.01$); 4-IPC (L) ($t = 2.061$, $P = 0.046$); and 5-IPC (R) ($t = 2.586$, $P = 0.014$) in RD patients. The sizes of the *spots* represent the degree of quantitative changes.

the information of the space position of the object and motion detection.

Our results indicated that rs-FC of RD patients was abnormal in DMN subregions at rest. In the default network of RD patients, paired regions of MTL.L-PCC, MTL.L-HF.L, MTL.L-HF.R, MTL.L-IPC.L, and MTL.L-IPC.R all had obvious functional impairment, and the degree of functional connection was significantly lower than that of the normal group, which provided a new area for us to study, the neural mechanism of visual cortex damage in RD patients, in the future.

The MTL is related to short-term memory and visual semantics of words. The PCC involves the advanced executive function of the human body. The spindle gyrus, the lower occipital gyrus, the occipital gyrus, the function of the wedge leaf and the lingual gyrus are related to vision, and the upper lobular/angular gyrus is an important part of the visual cognitive function. HF plays an important role in memory storage and reproduction, while RD caused by visual-related barriers is inextricably linked to MTL, PCC, and IPC. And our results also confirmed that their functional connections have changed significantly. However, Banich et al.[19] applied fMRI and found that MPFC might be important in controlling execution, and its activity form varies according to the content of the task. Our experiment did not discover the obvious changes of MPFC, which means that the function of MPFC might not have much influence on the vision.

The ROC curve has been used previously to distinguish disease from healthy subjects. The accuracy is considered perfect for AUC values between 0.7 and 0.9; the discrimination result is unreliable when AUC is 0.4 to 0.7. In this study, ROC curve analysis revealed that the AUCs of MTL.L-HF.R and MTL.L-IPC.R were over 0.7, which might indicate these specific FC differences have the sensitivity and specificity to identify RD. In brief, our research demonstrated that the DMN method might be an effective measurement method of the rs-fMRI, suggesting that the MTL.L-HF.R and MTL.L-IPC.R might be potential diagnostic markers for RD patients in the future.

However, this study also has limitations. Seeley et al.[20] found that the spontaneous activity of individuals was related to the anxiety of subjects before scanning. Although this study set up the control group, we could not completely exclude the impact of the mental status of the subjects due to the different circumstances of the subjects. Also, the patients in the RD group were operated on anesthesia. It has been found that varying degrees of spontaneous activity were observed in the resting state of the brain sedated with sevoflurane and midazolam.[21,22] Thus, we could not judge the extent of the effect of the anesthetics received by the subjects during the operation.

Conclusion

In summary, this study illustrated that the visual function changes of RD patients were closely related to the DMN functional connections. The FC of MTL, PCC, HF, and IPC were significantly changed, which provided insight into the neural variation in RD patients and assisted in revealing the potential mechanisms of RD.

Acknowledgments

Disclosure: **T. Su**, None; **Y.-Q. Shu**, None; **K.-C. Liu**, None; **L. Ye**, None; **L.-L. Chen**, None; **W.-Q. Shi**, None; **Y.-L. Min**, None; **X.-W. Xu**, None; **Q. Yuan**, None; **P.-W. Zhu**, None; **Y. Shao**, None

*Ting Su and Yong-Qiang Shu have contributed equally to this work.

References

1. Greicius MD, Krasnow B, Reiss AL, Menon V. Functional connectivity in the resting brain. *Proc Natl Acad Sci U S A*. 2003;100:253–258.
2. Friston KJ. Functional and effective connectivity: a review. *Brain Connect*. 2011;1:13–36.
3. Koyama MS, Martino AD, Zuo XN, et al. Resting-state functional connectivity indexes

reading competence in children and adults. *J Neurosci*. 2011;31:8617.

4. Guo W, Jiang J, Xiao C, et al. Decreased resting-state interhemispheric functional connectivity in unaffected siblings of schizophrenia patients. *Schizophr Res*. 2014;152:170–175.

5. Saad ZS, Gotts SJ, Murphy K, et al. Trouble at rest: how correlation patterns and group differences become distorted after global signal regression. *Brain Connect*. 2012;2:25–32.

6. Collins DL, Zijdenbos AP, Kollokian V, et al. Design and construction of a realistic digital brain phantom. *IEEE Trans Med Imaging*. 1998; 17:463–468.

7. Kiviniemi V, Kantola JH, Jauhiainen J, Tervonen O. Comparison of methods for detecting nondeterministic BOLD fluctuation in fMRI. *Magn Reson Imaging*. 2004;22:197–203.

8. Pennefather PM, Chandna A, Kovacs I, Polat U, Norcia AM. Contour detection threshold: repeatability and learning with 'contour cards.' *Spat Vis*. 1999;12:257–266.

9. Polat U, Bonneh Y. Collinear interactions and contour integration. *Spat Vis*. 2000;13:393–401.

10. Saarinen J, Levi DM. Integration of local features into a global shape. *Vision Res*. 2001;41:1785–1790.

11. Crewther DP, Crewther SG. Neural site of strabismic amblyopia in cats: spatial frequency deficit in primary cortical neurons. *Exp Brain Res*. 1990;79:615–622.

12. Shooner C, Majaj NJ, Kumbhani RD. Neural correlates of amblyopia in foveal and parafoveal visual cortex of amblyopic macaque monkeys. *J Vis*. 2014;14:689–689.

13. Kiorpes L, Kiper DC, O'Keefe LP, Cavanaugh JR, Movshon JA. Neuronal correlates of amblyopia in the visual cortex of macaque monkeys with experimental strabismus and anisometropia. *J Neurosc*. 1998;18:6411–6424.

14. Buzsáki G, Draguhn A. Neuronal oscillations in cortical networks. *Science*. 2004;304(5679):1926–1929.

15. Laufs H, Krakow K, Sterzer P, et al. Electroencephalographic signatures of attentional and cognitive default modes in spontaneous brain activity fluctuations at rest. *Proc Natl Acad Sci U S A*. 2003;100:11053–11058.

16. Schlösser R, Gesierich T, Kaufmann B, et al. Altered effective connectivity during working memory performance in schizophrenia: a study with fMRI and structural equation modeling. *Neuroimage*. 2003;19:751–763.

17. Raichle ME, MacLeod AM, Snyder AZ, Powers WJ, Gusnard DA, Shulman GL. A Default mode of brain function. *Proc Natl Acad Sci U S A*. 2001;98:676–682.

18. Gusnard DA, Raichle ME, Raichle ME. Searching for a baseline: functional imaging and the resting human brain. *Nat Rev Neurosci*. 2001;2: 685–694.

19. Banich MT, Milham MP, Atchley R, et al. fMRI studies of stroop tasks reveal unique roles of anterior and posterior brain systems in attentional selection. *J Cogn Neurosci*. 2000;12:988–1000.

20. Seeley WW, Menon V, Schatzberg AF, et al. Dissociable intrinsic connectivity networks for salience processing and executive control. *J Neurosci*. 2007;27:2349–2356.

21. Kiviniemi VJ, Haanpää H, Kantola JH, et al., Midazolam sedation increases fluctuation and synchrony of the resting brain BOLD signal. *Magn Reson Imaging*. 2005;23:531–537.

22. Peltier SJ, Kerssens C, Hamann SB, et al. Functional connectivity changes with concentration of sevoflurane anesthesia. *Neuroreport*. 2005; 16:285–288.